nature genetics

Germline mutations in breast and ovarian cancer pedigrees establish *RAD51C* as a human cancer susceptibility gene

Alfons Meindl[1], Heide Hellebrand[1,16], Constanze Wiek[2,16], Verena Erven[2], Barbara Wappenschmidt[3], Dieter Niederacher[4], Marcel Freund[2], Peter Lichtner[5], Linda Hartmann[6], Heiner Schaal[6], Juliane Ramser[1], Ellen Honisch[4], Christian Kubisch[7], Hans E Wichmann[8], Karin Kast[9], Helmut Deißler[10], Christoph Engel[11], Bertram Müller-Myhsok[12], Kornelia Neveling[13], Marion Kiechle[1], Christopher G Mathew[14], Detlev Schindler[13], Rita K Schmutzler[3,17] & Helmut Hanenberg[2,15,17]

Germline mutations in a number of genes involved in the recombinational repair of DNA double-strand breaks are associated with predisposition to breast and ovarian cancer. *RAD51C* is essential for homologous recombination repair, and a biallelic missense mutation can cause a Fanconi anemia–like phenotype. In index cases from 1,100 German families with gynecological malignancies, we identified six monoallelic pathogenic mutations in *RAD51C* that confer an increased risk for breast and ovarian cancer. These include two frameshift-causing insertions, two splice-site mutations and two nonfunctional missense mutations. The mutations were found exclusively within 480 pedigrees with the occurrence of both breast and ovarian tumors (BC/OC; 1.3%) and not in 620 pedigrees with breast cancer only or in 2,912 healthy German controls. These results provide the first unambiguous evidence of highly penetrant mutations associated with human cancer in a *RAD51* paralog and support the 'common disease, rare allele' hypothesis.

The breast cancer susceptibility genes *BRCA1*, *BRCA2*, *ATM*, *CHEK2*, *BRIP1* and *PALB2* are essential in the genomic stability of cells and have been functionally linked to the homologous recombination pathway of DNA repair[1,2]. Biallelic mutations in *BRCA2*, *PALB2* and *BRIP1* are viable and cause a rare childhood chromosomal instability disorder, Fanconi anemia (FA), characterized by developmental abnormalities, bone marrow failure and predisposition to leukemia and other cancers[3,4]. In an accompanying paper, we have identified a homozygous missense mutation (R258H) in *RAD51C* as the causal mutation in a family with three children severely affected by FA-typical birth defects[5]. Skin fibroblasts from the affected person showed cellular hypersensitivity to DNA cross-linking agents and had impaired RAD51 foci formation after DNA damage[5]. These features are typical hallmarks of FA cells with defects in *BRCA2* (*FANCD1*)[6] and *PALB2* (*FANCN*)[7,8] and reflect the essential role of FA proteins in homologous recombination repair[2,3,9]. Here we have assessed whether monoallelic germline alterations in *RAD51C* confer susceptibility to breast or ovarian cancer, or both, by screening the *RAD51C* gene in 1,100 affected individuals from pedigrees with gynecological cancers that were negative for mutations in *BRCA1* and *BRCA2*.

In total, we detected 14 germline sequence alterations in *RAD51C* in 1,100 unrelated affected women from pedigrees with hereditary breast cancer and BC/OC: two single–base pair insertions, two splice-site mutations and ten sequence alterations leading to single amino acid changes (**Table 1**). Three missense variants (A126T, G264S and T287A) were identified frequently in affected individuals from unrelated pedigrees and also in healthy German controls[10]; the remaining missense alterations were unique for the respective pedigree. **Figure 1** shows the extended family trees for eight sequence alterations, with the individuals depicted being at least 30 years of age. As only the two insertions—both leading to frame shift and premature protein termination (insertion 224_225insA causing Y75XfsX0, **Fig. 1a**, and 525_526insC leading to C176LfsX26, **Fig. 1b**)—were clearly pathogenic, we characterized the other germline alterations by *in vitro* functional tests.

[1]Department of Obstetrics and Gynecology, Division of Tumor Genetics, Klinikum rechts der Isar der Technischen Universitaet Muenchen, Munich, Germany. [2]Department of Pediatric Hematology, Oncology and Clinical Immunology, Children's Hospital, Heinrich-Heine-University, Düsseldorf, Germany. [3]Center for Familial Breast and Ovarian Cancer and Center for Integrated Oncology, University Hospital, Cologne, Germany. [4]Department of Obstetrics and Gynecology, Heinrich-Heine-University, Düsseldorf, Germany. [5]Institute of Human Genetics, Helmholtz Zentrum Muenchen, Neuherberg, Germany. [6]Institute of Virology, Heinrich-Heine-University, Düsseldorf, Germany. [7]Institute of Human Genetics, Center for Molecular Medicine Cologne and Cologne Excellence Cluster on Cellular Stress Response in Aging-Associated Diseases, University of Cologne, Cologne, Germany. [8]Institute of Epidemiology, Helmholtz Zentrum Muenchen, Neuherberg, Germany. [9]Department of Obstetrics and Gynecology, Carl Gustav Carus University, Dresden, Germany. [10]Department of Obstetrics and Gynecology, Ulm University, Ulm, Germany. [11]Institute for Medical Informatics, Statistics and Epidemiology, University of Leipzig, Leipzig, Germany. [12]Max-Planck-Institute of Psychiatry, Munich, Germany. [13]Department of Human Genetics, University of Würzburg, Würzburg, Germany. [14]Department of Medical and Molecular Genetics, Kings College, Guy's Hospital, London, UK. [15]Department of Pediatrics, Wells Center for Pediatric Research, Riley Hospital, Indiana University School of Medicine, Indianapolis, Indiana, USA. [16]These authors contributed equally to the work. [17]These authors contributed equally to the direction of the work. Correspondence should be addressed to A.M. (alfons.meindl@lrz.tu-muenchen.de) or H.H. (helmut.hanenberg@uni-duesseldorf.de).

Received 5 November 2009; accepted 22 March 2010; published online 18 April 2010; doi:10.1038/ng.569

Table 1 Mutations or variants in *RAD51C* identified through analyses of individuals with familial breast and/or ovarian cancer

			Predictive algorithms		Complementation of *Δ Rad51c* DT40 cells	Complementation of *RAD51C*-mutated fibroblasts	LOH in tumors			
Site	Nucleotide change	Protein change	SIFT[a]	PolyPhen[b]	Survival of cells	RAD51 foci	Cases	Breast cancer *n* = 620	BC/OC *n* = 480	Controls *n* = 2912
Ex 2	224_225insA	Y75XfsX0	–	–	–	–		0	1	0
Ex 3	525_526insC	C176LfsX26	–	–	–	–		0	1	0
IVS 1	145+1G>T	V15KfsX9	–	–	–	–	1/1	0	1	0
IVS 6	904+5G>T	V280GfsX11	–	–	–	–	2/2	0	1	0
Ex 2	G374T	G125V	Yes	Pb	No	No	4/4	0	1	0
Ex 3	G414C	L138F	Yes	Ps	No	Reduced	3/3	0	1	0
Ex 3	G475A	D159N	Yes	Ps	Reduced	Normal		1	0	0
Ex 9	G1097A	R366Q	Yes	Ps	Reduced	Normal	0/1	0	1	0
Ex 5	G790A	G264S	No	No	Reduced	Normal		3	9[c]	16[c]
Ex 6	A859G	T287A	No	Pb	Reduced	Normal		12	3	35
Ex 1	G7A	G3R	Yes	Pb	Normal	Normal	0/1	0	1	0[d]
Ex 2	G376A	A126T	No	No	Normal	Normal		13	3	8[d]
Ex 3	T506C	V169A	No	No	Normal	Normal		1	0	0[d]
Ex 6	G791T	G264V	No	Pb	Normal	Normal		1	0	0[d]

Ex, Exon; IVS, intervening sequence.
[a]SIFT: Yes, affects function; No, tolerated. [b]PolyPhen: Ps, possibly damaging; Pb, probably damaging; No, benign. [c]Odds ratio for BC/OC, 3.44; Confidence interval, 1.51–7.80; $P = 5.32 \times 10^{-3}$. [d]$n = 620$.

The splice donor mutation (145+1G>T) presents in a family with three sisters affected by breast or ovarian cancers (**Fig. 1c**) and disrupts the canonical GT dinucleotide. Comparison of the *RAD51C* splicing pattern in peripheral blood leukocytes from two heterozygous mutation carriers (**Fig. 2a**,**b**) revealed reduced expression of the normal *RAD51C*-001 and increased expression of the nonfunctional *RAD51C*-008 transcript, whereas levels of the nonfunctional *RAD51C*-009 transcript were unchanged compared to controls (transcripts and nomenclature according to the Ensembl genome browser). The latter two transcripts used alternative 5′ splice sites with intrinsic strengths of 17.4 and 16.1, respectively, as predicted by the HBond algorithm for 5′ splice sites[11] and confirmed by sequencing of the splice junctions in the different RT-PCR products (**Supplementary Fig. 1a**). To prove that the normal *RAD51C* transcript was expressed solely from the wild-type allele in the heterozygous leukocytes, we introduced exon 1, intron 1 and exon 2 of the *RAD51C* gene into a splicing construct[12]

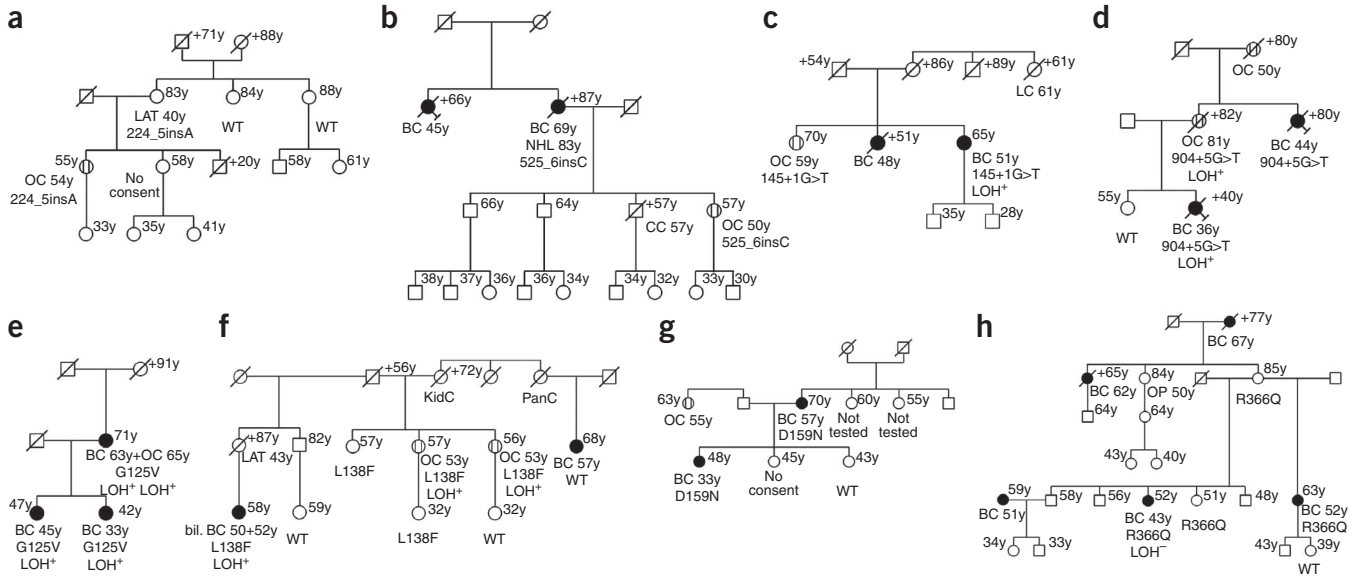

Figure 1 *RAD51C* mutations in familial breast and ovarian cancer pedigrees. (**a**–**h**) Individuals with breast cancer (BC) are shown as filled circles, females with ovarian cancer (OC) as streaked circles; OP, surgery. Disease and age in years (y) at first diagnosis is given underneath the symbol, current age or age at death (+) above it. Other cancers diagnosed in the pedigrees are also shown (LC, lung cancer; KidC, kidney cancer; PanC, pancreatic cancer; CC, colon cancer; LAT, lower abdominal tumor; NHL, non-Hodgkin lymphoma; bil., bilateral). All affected individuals with breast or ovarian cancer not tested for germline mutations in *RAD51C* were deceased or refused testing. Carriers of *RAD51C* mutations are shown with their specific *RAD51C* mutation (as listed in **Table 1**), whereas individuals who tested negative for the mutation in the specific pedigree are depicted as wild-type (WT). In addition, LOH data (+ for loss of the WT allele, – for a retained WT allele) is shown for the individuals for whom formalin-fixed, paraffin-embedded (FFPE) tissue samples of the tumor(s) could be analyzed.

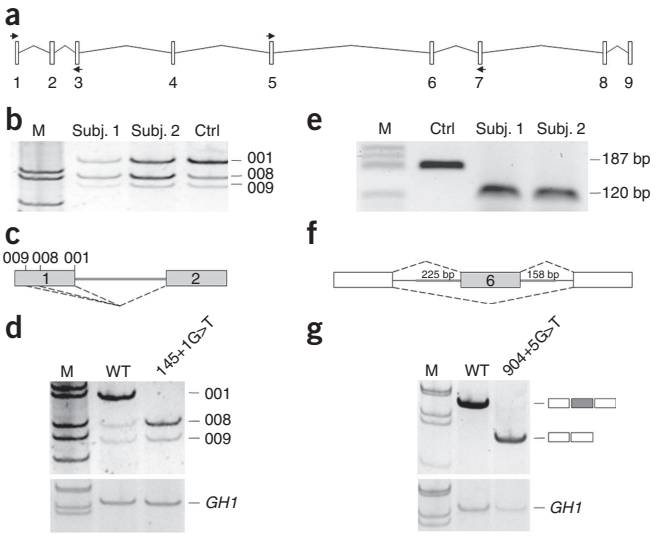

Figure 2 Functional analysis of the splice donor mutations 145+1G>T and 904+5G>T. (**a**) Structure of *RAD51C* transcript 001 (Ensembl ID OTTHUMT00000280540) and the primers for RT-PCR. (**b**) Using primers located in exon 1 and exon 3, we performed RT-PCR analysis of RNA from PB mononuclear cells of two affected individuals with breast or ovarian cancer (subj. 1, subj. 2) harboring the 145+1G>T splice donor mutation. This revealed three alternative transcripts from exon 1: *RAD51C*-001 and the two nonfunctional alternatively spliced transcript isoforms *RAD51C*-008 (Ensembl ID OTTHUMT00000280547) and *RAD51C*-009 (Ensembl ID OTTHUMT00000280548), as predicted by the HBond splice donor algorithm and confirmed by sequencing of the PCR products (**Supplementary Fig. 1a**). (**c**) Schematic drawing of the splice donor sites (GT) in *RAD51C* exon 1 used in transcripts *RAD51C*-001, *RAD51C*-008 and *RAD51C*-009, respectively. (**d**) RT-PCR analysis of HeLa cells transfected with *RAD51C* minigene splicing constructs carrying either the wild-type or the 145+1G>T mutant 5′ splice site showed complete inactivation of this mutated 5′ splice site and confirmed the differences in splicing pattern between heterozygous mutation carriers and normal controls shown in **b**. The cells were co-transfected with *growth hormone-1* (*GH1*) as a control. (**e**) RT-PCR analysis of RNA extracted from tumor samples from two carriers of the 905+5G>T mutation. Sequencing of the PCR products showed that these splice donor mutations led to exon 6 skipping (**Supplementary Fig. 1b**). (**f**) Schematic drawing of a three-exon splicing reporter containing *RAD51C* exon 6 with adjacent intronic sequences. (**g**) RT-PCR analysis of RNA from HeLa cells transfected with the minigene constructs revealed exclusion of exon 6 in the presence of the 905+5G>T mutation compared to the wild-type 5′ splice site.

(**Fig. 2c**). RT-PCR analysis after transfection of HeLa cells with the wild-type splicing reporter construct revealed usage of the exon 1 splice donor comparable to normal controls (**Fig. 2d**). In contrast, the RT-PCR analysis of the 145+1G>T splicing reporter showed complete inactivation of this mutant 5′ splice site and increased transcript levels from the upstream proximal 5′ splice site. Finally, the pathogenic nature of this 5′ splice site mutation was demonstrated by the loss of the wild-type allele in the cancer tissue of the surviving subject with breast cancer in pedigree 1C (**Supplementary Fig. 2a**).

The second splice site mutation (904+5G>T) also affected an evolutionarily conserved position and was predicted to greatly decrease the complementarity between the U1 small nuclear RNA and the 5′ splice site: the HBond score[11] decreased from 15.8 to 10.1, a predictor of aberrant splicing. As cells carrying the germline mutation were not available (**Fig. 1d**), mRNA was isolated from paraffin-embedded tumor samples from two carriers of this mutation. As shown in **Figure 2e**, we were able to specifically amplify an RT-PCR product that lacked exon 6 in these carriers (**Supplementary Fig. 1b**) but not in control samples. For further confirmation, we introduced the *RAD51C* exon 6 with flanking 225- and 158-bp intronic sequences into a splicing reporter construct[12] (**Fig. 2f**). Functional analysis in this heterologous context also demonstrated that the 904+5G>T mutation resulted in exclusion of exon 6, suggesting that the *RAD51C* exon 6 is recognized by exon definition (**Fig. 2g**). Finally, sequencing of DNA extracted from paraffin-embedded samples revealed that loss of the wild-type allele had occurred independently in the breast and the ovarian cancer tissues in two affected individuals from pedigree D (**Supplementary Fig. 2c**).

To initially screen whether the ten missense amino acid alterations change RAD51C protein function (**Fig. 3**), we used retroviral vectors[13] to introduce the mutant human RAD51C proteins (**Supplementary Fig. 3**) into chicken DT40 cells in which the *RAD51C* ortholog had been disrupted[14]. Survival of cells expressing two missense alterations at highly conserved amino acids, G125V and L138F (**Supplementary Fig. 4**), was identical to the survival of control vector-transduced or untransduced Δ*Rad51c* DT40 cells (**Fig. 3a**); the missense proteins therefore completely failed to complement the *Rad51c* mutant phenotype of these cells. In contrast, expression of the G3R, A126T, V169A and G264V missense *RAD51C* complementary DNAs corrected the mitomycin C (MMC) hypersensitivity of *Rad51c* mutant DT40 cells to levels achieved by expression of the wild-type *RAD51C* cDNA (**Fig. 3a**,**c**). Expression of the four missense alterations D159N, G264S, T287A and R366Q only partially restored the MMC sensitivity of Δ*Rad51c* DT40 cells compared to the wild-type cDNA (**Fig. 3b**,**c**) indicating hypomorphic mutations with reduced protein activity.

For further functional analysis of these missense mutations in human cells, we used the recently described *RAD51C*-mutated skin fibroblasts[5]. Assessing RAD51 foci[15–17] in these cells after cross-linker exposure revealed that expression of the two mutations G125V and L138F did not restore normal RAD51 foci formation (**Fig. 4**), whereas *RAD51C*-mutated cells transduced with vectors expressing the remaining eight *RAD51C* missense variants were functionally indistinguishable from cells expressing the wild-type *RAD51C* cDNA.

In total, six germline alterations in *RAD51C* were classified as pathogenic: the two insertions, the two splice site mutations and the two missense alterations G125V and L138F. The corresponding pedigrees are shown in **Figure 1a–f**. One amino acid change (D159N) that was associated with reduced survival in DT40 cells, albeit leading to normal RAD51 foci formation when the missense protein was expressed in human *RAD51C*-mutated cells, was considered as an unclassified variant, unique in this pedigree affected by breast cancer only (**Fig. 1g**). Finally, despite intermediate complementation in DT40 cells, predictions by algorithms and amino acid conservation in *RAD51C* homologs, the R366Q variant (**Fig. 1h**) appeared unlikely to be pathogenic, as segregation was incomplete and there was no loss of heterozygosity (LOH) in the tumor tested.

We tested whether the two recurrent missense mutations G264S and T287A, showing reduced survival of DT40 cells and normal RAD51 foci formation, were associated with cancer. Both G264S and T287A had no association with cancer in 1,100 affected individuals compared to 2,912 healthy controls. However, the G264S variant showed some evidence of association with malignancies in the subgroup of BC/OC families (**Table 1**; odds ratio, 3.44; confidence interval, 1.51–7.80; $P = 5.32 \times 10^{-3}$). Further assessment in larger studies is required to confirm this association.

The overall frequency of a pathogenic mutation in *RAD51C* among investigated families is 0.55% (6 of 1,100). However, when analyzing the six pedigrees with clearly pathogenic mutations (**Fig. 1a–f**), we

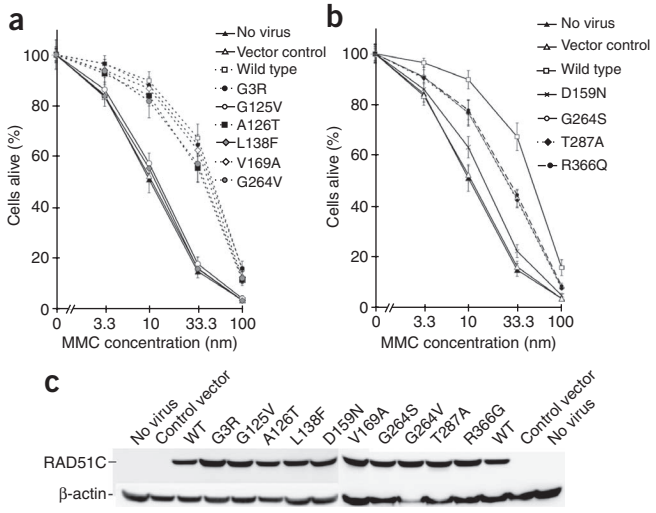

Figure 3 Function of *RAD51C* missense mutations in *Rad51c*-deficient DT40 cells. (**a**) Examining the survival of *Rad51c*-deficient DT40 cells with the mutant RAD51C proteins allowed us to distinguish mutants with normal function (G3R, A126T, V169A and G264V) from nonfunctional true null mutants (G125V and L138F). Also depicted are the survival curves for nontransduced (no virus) cells as well as cells transduced with either the control virus (vector control) or the wild-type *RAD51C* cDNA (wild-type or WT). Data shown are means ± s.d. from four different experiments. (**b**) Survival of *Rad51c*-deficient DT40 cells with the human RAD51C proteins having intermediate activity (D159N, G264S, T287A and R366Q; $n = 4$). Controls are as in **b**. Data shown are means ± s.d. from four different experiments. (**c**) Protein blot on puromycin-resistant *Rad51c*-deficient DT40 cells expressing the wild-type and the missense proteins of the retroviral long terminal repeat promoter shows equal expression of the mutant proteins.

observed that all pedigrees presented with both breast and ovarian cancers—over different generations, in siblings or even as metachronous tumors. Thus, the six clearly pathogenic *RAD51C* mutations were all found within the 480 BC/OC pedigrees (1.3%).

In these six *RAD51C*-associated German BC/OC pedigrees, the mean age of onset at first diagnosis was 53 years (range 33–78) for breast cancer and 60 years (range 50–81) for ovarian cancer. This is higher than the mean ages of 40 and 46 years for German BRCA1- and BRCA2-associated breast cancer, respectively, although lower than the mean age of 63 years for sporadic breast cancer. For ovarian cancer, the mean age of onset in individuals carrying *BRCA1* and *BRCA2* mutations and the general population is 49, 58 and 68 years, respectively (R.K.S., A.M. and the German Consortium for Hereditary Breast and Ovarian Cancer (GC-HBOC), unpublished data). No occurrence of male breast cancer was noted in these families. In addition, the segregation pattern in these six families is striking: none of the tested healthy females over 70 years of age inherited the mutations (the unaffected obligate carriers of the L138F mutation in **Fig. 1f** and of the frameshift mutation 224_5insA in **Fig. 1a** had surgery with removal of ovaries and uterus owing to a lower abdominal tumor at 43 and 40 years of age, respectively), and all of the affected first-degree relatives who developed malignancies and could be subjected to mutation analysis turned out to be carriers. This pattern of apparently complete segregation in the *RAD51C* families differs from that of families carrying *ATM*, *CHEK2*, *BRIP1* and *PALB2* mutations[1]. The occurrence of both breast and ovarian cancers, and the high frequencies, markedly resembles the clinical presentations of people carrying *BRCA1* and *BRCA2* mutations[1,18]. It is well established that the breast cancer histology in people with *BRCA1* mutations shows an excess of ductal tumors with high mitotic count and negativity for hormone receptors and HER2/neu, compared to individuals with *BRCA2* mutations or with sporadic breast cancers[19,20].

Pathology reports were available from 11 cases of breast cancer associated with pedigrees shown in **Figure 1a–f**. Ten were classified as invasive and one as preinvasive ductal carcinomas. Only three of the ten invasive cancers presented with lymph node infiltration. Three cases were high-grade (G3) and eight cases were intermediate-grade (G2) tumors. Hormone receptor status was available for ten tumors: five were negative and five positive for the estrogen and progesterone receptors (ER and PR). Of these, seven showed a concordant status: three were negative for both ER and PR, and four were positive for both ER and PR. Three tumors harbored a discordant receptor status: two were ER negative and PR positive, and one was ER positive and PR negative. All six breast cancers with HER2/neu status had a negative score. Of those, five were either ER or PR positive and one was negative for both receptors. These results indicate that *RAD51C*-associated breast cancer is distinct from *BRCA1*-associated breast cancer and might be associated with more favorable histopathological features like those of *BRCA2*-associated breast cancer. Pathological reports were available for seven *RAD51C*-associated ovarian cancers, six of which presented as invasive serous and one as invasive endometrioidal adenocarciomas. Three ovarian cancers were classified as high-grade (G3) and four as intermediate-grade (G2) tumors. Despite the fact that five of the seven ovarian cancers presented as pT3 tumors, only two had lymph node involvement, again indicating distinct features compared to *BRCA1*-associated ovarian cancers, the majority of which are poorly differentiated invasive serous adenocarcinomas[21].

Although *RAD51C* was identified in mammalian cells more than 10 years ago[22], our findings on germline mutations in BC/OC families and the accompanying report on the identification of *RAD51C* as a new FA-like gene[5] are, to our knowledge, the first clear links between mutations in *RAD51C* and human disease. According to the LOH in pedigrees shown in **Figure 1a–f** (**Supplementary Fig. 2**) and recent

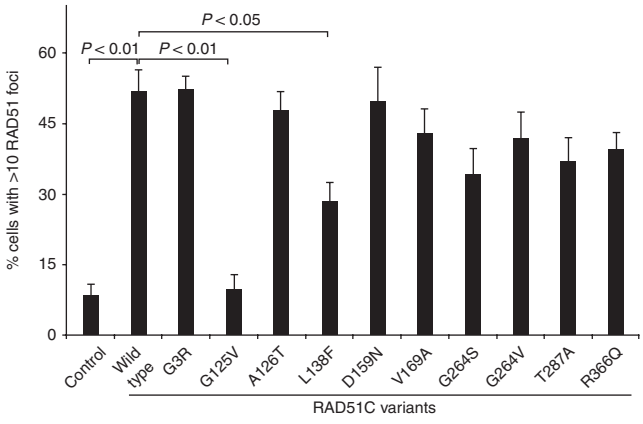

Figure 4 Function of RAD51C missense mutations in human *RAD51C*-mutated fibroblasts. We analyzed formation of RAD51 foci by immunofluorescent antibody staining in human *RAD51C*-mutated cells transduced with retroviral vectors that expressed each of the ten *RAD51C* missense alterations or the wild-type *RAD51C* cDNA. Shown are the percentages of cells (mean ± s.e.m.) with more than ten RAD51 foci after incubation for 24 h in 150 nM MMC, from three different experiments counted by two different people blinded for each condition. We assessed statistical significance by Student's *t*-test, applying SPSS software version 17.0; significance is indicated for G125V and L138F compared to the wild-type control.

experiments with conditional knockouts in mice[23], *RAD51C* functions as TP53-dependent tumor suppressor gene. The well-known association of genetic risk factors for breast and ovarian cancers with FA suggests that sequencing studies of FA genes and their protein interaction partners might reveal the existence of additional cancer susceptibility genes in the FA/BRCA pathway of homologous recombination repair[24]. In addition, the high penetrance of mutations impairing RAD51C function, and the causative link with the occurrence of gynecological cancers, justifies testing of other malignancies[25] for alterations in *RAD51C* and its paralog. Ultimately, the identification of *RAD51C* as cancer susceptibility gene supports the 'common disease, rare allele' hypothesis[26], suggesting that affected females with a strong history for breast and ovarian cancer, but negative for mutations in *BRCA1*, *BRCA2* and also *RAD51C*, should be screened using exomic sequencing[25].

METHODS

Methods and any associated references are available in the online version of the paper at http://www.nature.com/naturegenetics/.

Note: Supplementary information is available on the Nature Genetics website.

ACKNOWLEDGMENTS

We thank all the families for providing samples for this study. We are deeply indebted to German Cancer Aid for establishing the GC-HBOC and their longstanding patronage. This work was supported by grants from the German Cancer Aid (grant numbers 107054 and 107353), the Juergen-Manchot-Stiftung (L.H., H.S.), the Cancer Society Northrhine-Westphalia (D.N., E.H., H.S.), the Forschungskommission of the Heinrich-Heine-University, Düsseldorf (M.F., D.N., H.S., H. Hanenberg), the Bundesministerium für Bildung und Forschung network for Inherited Bone Marrow Failure Syndromes (H.S., H. Hanenberg) and the Deutsche Forschungsgemeinschaft SPP1230 (H. Hanenberg). We also thank N. Arnold, C. Bartram, U. Bick, W. Diestler, M. Loeffler, T. Grimm, R. Kreienberg, C. Nestle-Kraemling, B. Schlegelberger and P. Wieacker for their long-standing collaboration within the GC-HBOC. Finally, we acknowledge the excellent technical assistance of B. Kau, G. Krebsbach, J. Koehler, W. Kuss, R. Friedl and S. Engert.

AUTHOR CONTRIBUTIONS

The study was designed by A.M., R.K.S. and H. Hanenberg. The screening experiments were performed by H. Hellebrand, D.N., B.W., K.K., H.D. and E.H. under the direction of A.M. Cloning, virus production, transductions and functional complementation tests were set up by C.W., V.E., K.N. and M.F. under the direction of H. Hanenberg and D.S. L.H. and H.S. performed splicing experiments. MALDI-TOF experiments were performed by P.L. under the direction of H.E.W. The statistical analyses were done by B.M.-M., R.K.S. and C.E. C.E. also provided clinical and histopathological data. Control samples were collected by C.K. and H.E.W. The search for families was initiated by M.K. and R.K.S., and families were provided by the GC-HBOC. J.R. and C.G.M. participated in discussing and revising the manuscript. The manuscript was written by A.M., R.K.S., D.N. and H. Hanenberg.

COMPETING FINANCIAL INTERESTS

The authors declare no competing financial interests.

Published online at http://www.nature.com/naturegenetics/.
Reprints and permissions information is available online at http://npg.nature.com/reprintsandpermissions/.

1. Turnbull, C. & Rahman, N. Genetic predisposition to breast cancer: past, present, and future. *Annu. Rev. Genomics Hum. Genet.* **9**, 321–345 (2008).
2. Ciccia, A., McDonald, N. & West, S.C. Structural and functional relationships of the XPF/MUS81 family of proteins. *Annu. Rev. Biochem.* **77**, 259–287 (2008).
3. Wang, W. Emergence of a DNA-damage response network consisting of Fanconi anaemia and BRCA proteins. *Nat. Rev. Genet.* **8**, 735–748 (2007).
4. Neveling, K., Endt, D., Hoehn, H. & Schindler, D. Genotype-phenotype correlations in Fanconi anemia. *Mutat. Res.* **668**, 73–91 (2009).
5. Vaz, F. *et al.* Mutation of the *RAD51C* gene in Fanconi anemia. *Nat. Genet.* advance online publication, doi:10.1038/ng.570 (18 April 2010).
6. Howlett, N.G. *et al.* Biallelic inactivation of BRCA2 in Fanconi anemia. *Science* **297**, 606–609 (2002).
7. Reid, S. *et al.* Biallelic mutations in PALB2 cause Fanconi anemia subtype FA-N and predispose to childhood cancer. *Nat. Genet.* **39**, 162–164 (2007).
8. Xia, B. *et al.* Fanconi anemia is associated with a defect in the BRCA2 partner PALB2. *Nat. Genet.* **39**, 159–161 (2007).
9. Thacker, J. The RAD51 gene family, genetic instability and cancer. *Cancer Lett.* **219**, 125–135 (2005).
10. Arking, D.E. *et al.* A common genetic variant in the NOS1 regulator NOS1AP modulates cardiac repolarization. *Nat. Genet.* **38**, 644–651 (2006).
11. Freund, M. *et al.* A novel approach to describe a U1 snRNA binding site. *Nucleic Acids Res.* **31**, 6963–6975 (2003).
12. Betz, B. *et al.* Comparative in silico analyses and experimental validation of novel splice site and missense mutations in the genes MLH1 and MSH2. *J. Cancer Res. Clin. Oncol.* published online (8 August 2009).
13. Hanenberg, H. *et al.* Colocalization of retrovirus and target cells on specific fibronectin fragments increases genetic transduction of mammalian cells. *Nat. Med.* **2**, 876–882 (1996).
14. Takata, M. *et al.* Chromosome instability and defective recombinational repair in knockout mutants of the five Rad51 paralogs. *Mol. Cell. Biol.* **21**, 2858–2866 (2001).
15. Badie, S. *et al.* RAD51C facilitates checkpoint signaling by promoting CHK2 phosphorylation. *J. Cell Biol.* **185**, 587–600 (2009).
16. Liu, Y., Masson, J.Y., Shah, R., O'Regan, P. & West, S.C. RAD51C is required for Holliday junction processing in mammalian cells. *Science* **303**, 243–246 (2004).
17. Katsura, M. *et al.* The ATR-Chk1 pathway plays a role in the generation of centrosome aberrations induced by Rad51C dysfunction. *Nucleic Acids Res.* **37**, 3959–3968 (2009).
18. King, M.C., Marks, J.H. & Mandell, J.B. Breast and ovarian cancer risks due to inherited mutations in BRCA1 and BRCA2. *Science* **302**, 643–646 (2003).
19. Lakhani, S.R. *et al.* Multifactorial analysis of differences between sporadic breast cancers and cancers involving BRCA1 and BRCA2 mutations. *J. Natl. Cancer Inst.* **90**, 1138–1145 (1998).
20. Lakhani, S.R. *et al.* Pathology of ovarian cancers in BRCA1 and BRCA2 carriers. *Clin. Cancer Res.* **10**, 2473–2481 (2004).
21. Lakhani, S.R. *et al.* Prediction of BRCA1 status in patients with breast cancer using estrogen receptor and basal phenotype. *Clin. Cancer Res.* **11**, 5175–5180 (2005).
22. Dosanjh, M.K. *et al.* Isolation and characterization of RAD51C, a new human member of the RAD51 family of related genes. *Nucleic Acids Res.* **26**, 1179–1184 (1998).
23. Kuznetsov, S.G., Haines, D.C., Martin, B.K. & Sharan, S.K. Loss of *Rad51c* leads to embryonic lethality and modulation of *Trp53*-dependent tumorigenesis in mice. *Cancer Res.* **69**, 863–872 (2009).
24. Thomas, G. *et al.* A multistage genome-wide association study in breast cancer identifies two new risk alleles at 1p11.2 and 14q24.1 (RAD51L1). *Nat. Genet.* **41**, 579–584 (2009).
25. Jones, S. *et al.* Exomic sequencing identifies PALB2 as a pancreatic cancer susceptibility gene. *Science* **324**, 217 (2009).
26. Walsh, T. & King, M.C. Ten genes for inherited breast cancer. *Cancer Cell* **11**, 103–105 (2007).

ONLINE METHODS

Subjects, families and pedigrees. We recruited affected individuals from 1,100 German pedigrees with hereditary gynecological malignancies through a clinicogenetic counseling program at five centers (Cologne, Dresden, Düsseldorf, Munich and Ulm) from the GC-HBOC[27,28]. Of these, 620 pedigrees fulfilled the criterion that at least three affected females with breast cancer but no ovarian cancers were present (breast cancer pedigrees). In 480 pedigrees, at least one case of breast and one ovarian cancer had occurred (BC/OC pedigrees)[28]. We checked that all affected individuals in this study did not carry pathogenic germline mutations in *BRCA1* and *BRCA2* using the PCR-based mutation-detection techniques dHPLC (or direct DNA sequencing, or both)[27] and multiplex ligation-dependent probe amplification[28]. In total, 2,912 age-matched control samples from healthy women were collected in Northrhine-Westphalia or provided by Kooperative Gesundheitsforschung in der Region Augsburg[10,29,30]. We completely sequenced 480 samples and screened 2,432 samples with matrix-assisted laser desorption/ionization–time of flight (MALDI-TOF; see below). Informed consent was obtained from all people participating in the study, and the experiments were approved by the ethics committee of the University of Cologne on behalf of the GC-HBOC.

Direct sequencing and dHPLC. For the rapid and reliable identification of *RAD51C* mutations, we used two different approaches. We detected mutations by dHPLC (WAVE system, Transgenomic) or by direct DNA sequencing on ABI3100 sequencers (Applied Biosystems). Primer pairs used for the amplification of the nine exons of the *RAD51C* gene are shown in **Supplementary Table 1**. Appropriate dHPLC conditions for running temperatures and buffer gradients were established for each individual exon. ABI BigDye terminator chemistry (Applied Biosystems) was used for cycle sequencing. We confirmed all mutations detected by DHPLC by direct DNA sequencing.

Sequencing of *RAD51C* transcripts. We amplified *RAD51C* transcripts from peripheral blood mononuclear cells by RT-PCR with primers for *RAD51C* exon 1 and exon 3 and separated them on 6% polyacrylamide gels. RT-PCR products were extracted with elution buffer (0.5 M ammonium acetate, 10 mM magnesium acetate, 1 mM EDTA, 0.1% SDS), reamplified with the RT-PCR primers using 2.5 U Pwo DNA polymerase (Roche Molecular Biochemicals), gel-extracted (gel extraction kit, Qiagen) and directly sequenced.

MALDI-TOF and statistics. We used the homogeneous mass-extension process for producing primer extension products analyzed on a MALDI-TOF mass spectrometer (Sequenom MassArray system)[31]. Assays were designed with the SpectroDesigner software. Primer sequences are available upon request.

We calculated *P* values from standard χ^2 tests on the basis of allele counts, and odds ratios using standard methods. All calculations were done using R 2.91.

RNA extraction. We isolated total RNA from paraffin-embedded tumor samples using the RNeasy FFPE kit (Qiagen), obtaining intact RNA molecules about 150 nucleotides long. We used PAXgene Blood RNA tubes for collection and stabilization of blood samples from subjects and isolated total RNA from blood samples with the PAXgene Blood RNA kit according to the manufacturer's instructions (PreAnalytiX, Qiagen).

Splicing analysis. We performed RT-PCR with total RNA extracted from blood samples derived from affected individuals. For analysis of the splicing pattern, before reverse transcription, 3 μg of total RNA was subjected to DNase I digestion with 10 U of DNase I (Roche Molecular Biochemicals). We reverse-transcribed 3 μl of the treated RNA samples with the SuperScript III RT-PCR System with Platinum Taq Polymerase (Invitrogen) using primer pairs specific for *RAD51C* exon 1 and exon 3, listed in **Supplementary Table 1**. To ensure a linear PCR amplification range allowing semiquantitative assessment of the spliced products, we performed PCR analysis with 28 cycles. PCR products were separated on 6% nondenaturing polyacrylamide gels, stained with ethidium bromide, visualized and quantified with the Lumi-Imager F1 (Roche Molecular Biochemicals) and directly sequenced after gel extraction.

Splicing reporter assays. For testing the 145+1G>T mutation, we amplified the subgenomic region spanning *RAD51C* exon 1, intron 1 and exon 2 from control DNA by PCR with primers listed in **Supplementary Table 1** using Expand High-Fidelity DNA Polymerase (Roche Molecular Biochemicals). We cloned the PCR product into the pSVT7 expression vector[32] and confirmed it by sequencing. We introduced the 5′ splice site mutation by PCR mutagenesis using the *RAD51C* intron 1 forward and reverse mutagenesis primers with the QuickChange XL Site-Directed Mutagenesis Kit (Stratagene). For functional analysis of the 904+5G>T mutation, we amplified the *RAD51C* exon 6, including the flanking intronic sequences, from genomic DNA by PCR with Expand High Fidelity DNA Polymerase and inserted it into the splicing reporter construct as described previously[12]. We inserted the mutation by PCR mutagenesis using the RAD51C intron 6 forward and reverse mutagenesis primers. Cell culture and transfection experiments were performed as previously described[32]. We isolated total RNA 30 h after transfection using the GenElute Mammalian Total RNA Miniprep kit (Sigma) and reverse-transcribed 200 ng of the DNase I (Roche Molecular Biochemicals)–treated RNA with the SuperScript III RT-PCR System with Platinum Taq Polymerase (Invitrogen) and vector-specific primers.

Loss-of-heterozygosity analysis. We extracted DNA from sections of paraffin-embedded tumor tissues (QIAamp DNA FFPE tissue kit, Qiagen) after macrodissection to ensure the amount of tumor cells > 80% as visualized in a hematoxylin and eosin–stained control section. We specifically amplified *RAD51C* DNA fragments using appropriate primer pairs listed in **Supplementary Table 1**, directly sequenced them with ABI sequencer 3130XL and compared them to sequencing results of heterozygous germline DNA.

Complementation of *Rad51c*-deficient DT40 cells. *Rad51c*-deficient DT40 cells[14] were purchased from the Riken BRC Cell Bank (Tsukuba). The control vectors S11IP, expressing an IRES-*pac* cassette, and S11RCIP, additionally expressing the wild-type *RAD51C* cDNA from the same expression cassette (**Supplementary Fig. 4**), were constructed as described[5]. We introduced the subject-derived missense mutations in the *RAD51C* open reading frame using a Quick Mutagenesis kit (Stratagene) according to the manufacturer's instructions. Generation of stable oncoretroviral cell lines and transduction of the nonadherent Δ*Rad51c* DT40 cells with retroviral supernatant were performed as previously described[13,33,34]. Transduced cells were selected in the presence of puromycin (Gibco/Invitrogen) for 4–5 d, exposed for 3 d to increasing concentrations of MMC and then assayed by flow cytometry for survival of cells; we used propidium iodide (Sigma-Aldrich) to discriminate live cells from dead cells as described[34].

Protein expression of *Rad51c* missense mutants in Δ*Rad51c* DT40 cells. We performed immunoblots with samples containing 50 μg of total protein on 4–12% NuPage Bis-Tris polyacrylamide gels (Invitrogen). Membranes were probed with mouse monoclonal anti-human RAD51C (1:1,000; ab55728 Abcam) or mouse monoclonal anti–β-actin (1:5,000; A2228 Sigma-Aldrich). We used a secondary horseradish peroxidase–linked sheep anti-mouse IgG (RPN4201 GE Healthcare) at a dilution of 1:10,000 and detected it by the chemiluminescence technique using the ECL system (Pierce, Thermo Fisher Scientific).

RAD51 foci immunofluorescence. For indirect immunofluorescence staining of RAD51 foci, we seeded cells onto coverslips (Nalgene NUNC) and incubated them the next day with 150 nM MMC (Medac) as described previously[35]. After 24 h, cells were fixed with 3.7% paraformaldehyde (Sigma-Aldrich) for 15 min at 20–25 °C and permeabilized with 0.5% (vol/vol) Triton X-100 for 5 min. After 30 min in blocking buffer (10% (wt/vol) BSA (PAA), 0.1% (vol/vol) NP-40 (Sigma-Aldrich)), cells were incubated at 4 °C with rabbit anti-RAD51 (PC130, Calbiochem) at 1:200 dilution for 45 min. Cells were washed three times in TBS (Invitrogen) and then incubated with a 1:500-diluted Texas Red–conjugated polyclonal anti-rabbit (Jackson Immunoresearch). After 45 min, cells were washed three times with TBS and the slides were mounted in ProLong Gold antifade reagent (Invitrogen) with 4,6-diamidino-2-phenylindole (DAPI, Sigma-Aldrich). We viewed specimens with an inverted microscope (Axiovert 200M, Zeiss) and fluorescence imaging workstation and acquired images at 20–25 °C with a Plan-Apochromat ×63, 1.4 numerical aperture oil immersion lens using a digital camera (AxioCam MRm, Zeiss). RAD51 foci were counted independently in three different

experiments by two different people, blinded for each condition. Statistical analysis was performed using the SPSS software.

URLs. Ensembl genome browser, http://www.ensembl.org/. R, http://cran.r-project.org/.

27. Meindl, A. & German Consortium for Hereditary Breast and Ovarian Cancer Comprehensive analysis of 989 patients with breast or ovarian cancer provides BRCA1 and BRCA2 mutation profiles and frequencies for the German population. *Int. J. Cancer* **97**, 472–480 (2002).
28. Engert, S. *et al.* MLPA screening in the BRCA1 gene from 1,506 German hereditary breast cancer cases: novel deletions, frequent involvement of exon 17, and occurrence in single early-onset cases. *Hum. Mutat.* **29**, 948–958 (2008).
29. Holle, R., Happich, M., Lowel, H. & Wichmann, H.E. KORA–a research platform for population based health research. *Gesundheitswesen* **67** (Suppl. 1), S19–S25 (2005).
30. Wichmann, H.E., Gieger, C. & Illig, T. KORA-gen–resource for population genetics, controls and a broad spectrum of disease phenotypes. *Gesundheitswesen* **67** (Suppl. 1), S26–S30 (2005).
31. Tang, K. *et al.* Chip-based genotyping by mass spectrometry. *Proc. Natl. Acad. Sci. USA* **96**, 10016–10020 (1999).
32. Freund, M. *et al.* Extended base pair complementarity between U1 snRNA and the 5′ splice site does not inhibit splicing in higher eukaryotes, but rather increases 5′ splice site recognition. *Nucleic Acids Res.* **33**, 5112–5119 (2005).
33. Hanenberg, H. *et al.* Optimization of fibronectin-assisted retroviral gene transfer into human CD34+ hematopoietic cells. *Hum. Gene Ther.* **8**, 2193–2206 (1997).
34. Hanenberg, H. *et al.* Phenotypic correction of primary Fanconi anemia T cells from patients with retroviral vectors as a diagnostic tool. *Exp. Hematol.* **30**, 410–420 (2002).
35. Rio, P. & Hanenberg, H. Functional knock-down of human RAD51 for testing the Fanconi anemia-BRCA connection. in *Fanconi Anemia: A Paradigmatic Disease for the Understanding of Cancer and Aging* (eds. Schindler, D. & Hoehn, H.) 211–225 (Karger, Basel, Switzerland, 2007).

doi:10.1038/ng.569